Inorganic Chemistry

Article

pubs.acs.org/IC

Systematic Study of the Luminescent Europium-Based Nonanuclear Clusters with Modified 2-Hydroxybenzophenone Ligands

Bin Zhang, Ting Xiao, Chunmei Liu, Qian Li, Yanyan Zhu, Mingsheng Tang, Chenxia Du,* and Maoping Song*

The College of Chemistry and Molecular Engineering, Zhengzhou University, Zhengzhou, 450052, P. R. China

Supporting Information

ABSTRACT: The reaction of 2-hydroxybenzophenone derivatives with europium ions has afforded a new family of luminescent nonanuclear Eu(III) clusters. Crystal structure analysis of the clusters reveals that the metal core comprises two vertex-sharing square pyramidal units. Most of these complexes show emissions typical of Eu^{3+} ion under visible light excitation (400−420 nm) at room temperature. Photophysical characterization and DFT study reveal a correlation between luminescent efficiencies of Eu(III) complexes and the electronic features of the ligands, which can be tuned by the nature of substituents in the 4-position of the ligands. The ligands with a fluorine substituent possess more suitable triplet energy levels, resulting in more intensive luminescence.

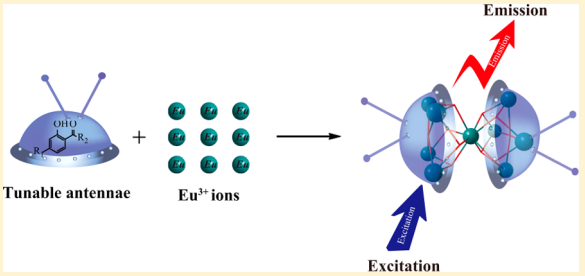

INTRODUCTION

Lanthanide-based high-nuclearity clusters have attracted considerable attention in recent years, not only for their aesthetically pleasing structures but also because of their intrinsic properties.[1] From the perspective of applications, envisioned or realized, polynuclear lanthanide complexes have shown promising results. For example, unique magnetic properties of certain lanthanide hydroxide clusters have been demonstrated in the form of single-molecule magnets[2] and long-lived and narrow emission bands ranging from near-infrared to visible regions of the complexes with lanthanide-hydroxo core have also been observed in cluster−polymer hybrid thin films.[3] However, the construction of polynuclear lanthanide complexes remains a great challenge ascribing to their variable and high coordination numbers as well as adventitious hydrolysis of the metal ions.[4] To date, the most successful synthetic route to single-sized lanthanide hydroxide clusters is the ligand-controlled hydrolytic approach which is exemplified by clusters stabilized by diketonate ligands.[5] A careful analysis of the supporting ligands used for various lanthanide-based clusters suggests that the ancillary ligand should present (i) easily accessible chelation regions to bind the Ln(III) ions and (ii) proper steric hindrance to bridge metal centers but prevent polymer formation.[6] Despite extensive attempts aimed at producing lanthanide oxido/hydroxido clusters, only a few kinds of bridging ligands have been successfully used for this purpose until now.[7] Thus, research activities in pursuing novel lanthanide clusters are of fundamental interest and practical significance.

Europium based oxido/hydroxido clusters featuring luminescence are of particular significance because of the intrinsic long-lived, sharp band red emission of Eu^{3+} ions,[8] which are highly pursued as phosphors in full-color display and as luminescent tags for biological molecules.[9] It is well-known that luminescence from trivalent europium arises from electronic transitions between the 4f orbitals, which are forbidden on symmetry grounds. Consequently, the use of chromophore ligands with strong light harvesting is necessary for efficient sensitizing of the Eu^{3+} ion through intramolecular energy transfer.[10] For highly luminescent Eu(III) complexes, the chelating ligands should have suitable triplet energy levels to match the $^5D_1$ or $^5D_0$ level of Eu^{3+} ion.[11] In fact, only a few kinds of ligands have been successfully used for producing luminescent europium oxido/hydroxido clusters with precisely defined structures until now.[12] In order to investigate the influence of supporting ligands on the structural patterns and luminescent behaviors of the clusters, it is of great importance to systematically explore new chelating ligands for optimizing sensitization processes in luminescent europium clusters. The 2-hydroxybenzophenone derivatives have been demonstrated to be good antennae for Eu^{3+} ion luminescence.[13] Their energy levels of the triplet states can be fine-tuned by incorporating substitutions into the ligands, which can result in more efficient intramolecular energy transfer in terms of ligand (S_1) → ligand (T_1) → Ln(III)*. Of particular significance, this kind of ligands shows great potential to stabilize the oxo and hydroxo components of the metal core, due to the good affinity in bridging europium ions through oxo and hydroxo groups and the proper steric hindrance to prevent the core from further aggregation. However, europium clusters with 2-hydroxybenzophenone derivatives as supporting ligands are rarely reported until now, especially for the high-nuclearity clusters.[14] With all of the above in mind, we extended our interests to design and

Received: May 14, 2013

   dx.doi.org/10.1021/ic401191e | Inorg. Chem. XXXX, XXX, XXX−XXX

synthesize novel high-nuclearity europium clusters with this kind of ligands. In this paper, we report six novel diabolo-shaped Eu_9 clusters assembled by two square pyramidal pentanuclear units via the apical metal center Eu(III) ion. The complexes with a general core of $[Eu(III)_9(L)_{16}(\mu_3\text{-}OH)_8(\mu_4\text{-}O)(\mu_4\text{-}OH)]$ have been confirmed by single-crystal X-ray diffraction, infrared (IR) spectroscopy, and elemental analysis (C, H, and N). The photophysical properties of the ligands and complexes have been thoroughly investigated, which shows that the substituents on the ligands play an important role for optimizing the ligand-to-europium energy transfer process. Quantum chemical calculations were conducted to help better understand the experimental results.

RESULTS AND DISCUSSION

Synthesis of the Ligands and Complexes. A series of 2-hydroxybenzophenone derivatives have been employed to investigate the effect of substituents on the photophysical properties of the europium clusters (Scheme 1). Ligands HL1–HL4 were purchased from Alfa Aesar company without further purification. The ligands of (4-fluoro-2-hydroxyphenyl)-phenylmethanone (HL5) and (4-fluoro-2-hydroxyphenyl)-(4-methlphenyl)methanone (HL6) were synthesized by a similar procedure according to the literature (Scheme 2).[15] Moderate yields for both ligands were obtained after column chromatography, ranging from 79% for HL5 to 72% for HL6, respectively.

Scheme 1. Diagram of α-Hydroxybenzophenone Derivatives

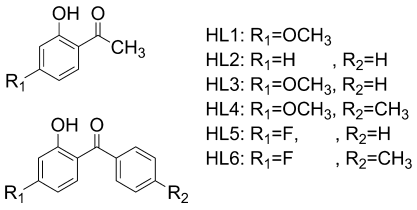

Scheme 2. Synthetic Pathway of the Ligands HL5 and HL6 (TEA: Triethylamine)

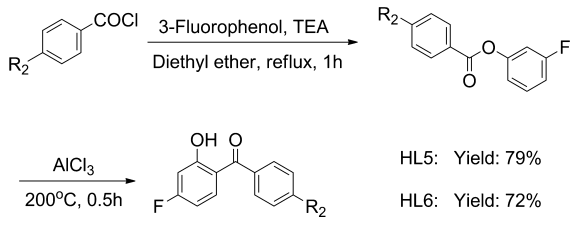

The procedure employed in the synthesis of the series of nonanuclear clusters relies on the reaction of 1 equiv of europium salt, $EuCl_3{\cdot}xH_2O$, with 2 equiv of the HL ligand in methanol using excess triethylamine as base. It seems that the relative small steric hindrance of these ligands and their good affinity for chelating and bridging Eu(III) ions may play an essential role in forming and stabilizing the nonanuclear metal clusters. In such cases, the L^- anions preoccupy part of the coordination sphere of the bulky lanthanide ions with $\mu_2{:}\eta^2$ coordination mode, leaving only a limited number of sites available for aqua coordination. As a result, deprotonation of the lanthanide-activated aqua ligands upon pH increase will be limited, and lead eventually to the well-defined polynuclear lanthanide clusters rather than the intractable and undesirable precipitates of lanthanide oxides or hydroxides. Then, a series of new europium oxido/hydroxido clusters of general core $[Eu(III)_9(L)_{16}(\mu_3\text{-}OH)_8(\mu_4\text{-}O)(\mu_4\text{-}OH)]$ were formed. This synthetic procedure is schematically illustrated in Scheme 3

Scheme 3. Rationales of the Ligand-Controlled Hydrolytic Approach to Assembly of the Clusters (Eu9-3)

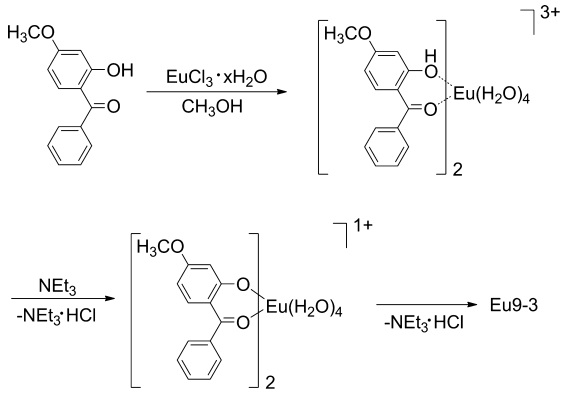

(Eu9-3 as an example). In the following sections, the europium(III) complexes based on HL1, HL2, HL3, HL4, HL5, and HL6 will be abbreviated as Eu9-1, Eu9-2, Eu9-3, Eu9-4, Eu9-5, and Eu9-6, respectively.

Crystal Structure Descriptions. The full data collections and the refinements of the structures have been done for Eu9-1, Eu9-3, Eu9-4, and Eu9-6, while only the cell parameters have been determined to confirm the structure of Eu9-2 due to the low crystallinity (Table S1 in the Supporting Information). X-ray diffraction analysis reveals that the four compounds are all nonanuclear clusters with a similar core structure (Figure S1, Supporting Information), although they are different in crystallography. Each core can be viewed as two vertex-sharing square pyramids arranged in a "staggered" fashion with their basal planes rotated by 45° with respect to each other (Figure S2, Supporting Information). The only difference of these complexes lies in that there are no solvent molecules in the asymmetric units of Eu9-3, Eu9-4, and Eu9-6, while Eu9-1 contains two water and two methanol molecules with a formula of $[Eu(III)_9(L_1)_{16}(\mu_3\text{-}OH)_8(\mu_4\text{-}O)(\mu_4\text{-}OH)]{\cdot}2H_2O{\cdot}2CH_3OH$. Thus, only the structure of the Eu9-3 cluster is briefly described as a representative.

X-ray crystal diffraction reveals that compound Eu9-3 consists of a nonanuclear $[Ln_9(\mu_4\text{-}O)(\mu_4\text{-}OH)(\mu_3\text{-}OH)_8]$ core and 16 deprotonated peripheral HL3 ligands. Selected bond lengths and angles for the complex Eu9-3 are listed in Table S2 in the Supporting Information. As shown in Figure 1, the molecular structure of Eu9-3 can be viewed as two $[Eu_5]$ clusters with Eu(1,2,3,4) forming the basal planes and the central Eu(5) atom as the shared apex. The coordination environment around the Eu(5) ion at the vertex is an almost perfect square antiprism by connecting with eight μ_3-bridging hydroxo groups. The bond lengths of Eu–O range from 2.455(2) to 2.472(2) Å, comparable to those in the reported Eu complex.[16] Each basal Eu(III) ion is eight-coordinate by two μ_3-OH, one μ_4-(O, OH), and five oxygen atoms from deprotonated HL3 ligands through chelating/bridging modes, forming a distorted square antiprism geometry.[17] The average bond length of Eu–(μ_4-(O, OH)) (2.597(3) Å) is apparently longer than that of Eu–(μ_3-OH) (2.351(3) Å), while the average bond length of Eu–O(phenolic group) (2.379(3) Å) is

dx.doi.org/10.1021/ic401191e | Inorg. Chem. XXXX, XXX, XXX–XXX

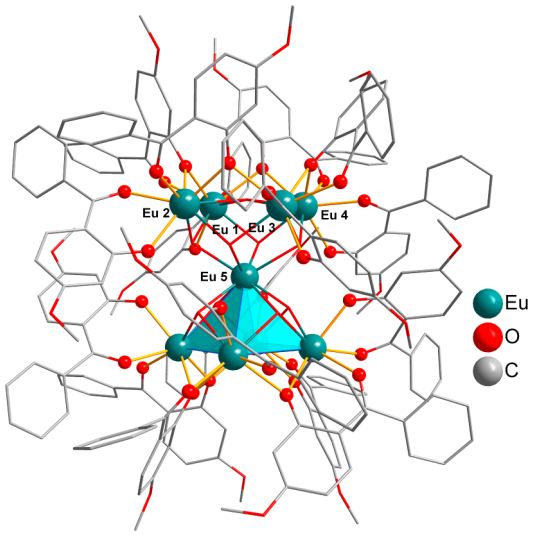

Figure 1. Molecular structure of the Eu9-3 cluster. For clarity, hydrogen atoms have been omitted.

shorter than that of Eu−O(carbonyl group) (2.387(3) Å). In the basal plane, four Eu(III) ions form a square-planar geometry with adjacent Eu···Eu distances ranging from 3.6515(3) to 3.6648(3) Å.

It is worth noting that, whatever ligands are used, the final compounds are all nonanuclear clusters in this system. The obvious tendency and recurrence of forming nonanuclear lanthanide−hydroxo cluster cores suggests that such a kind of ancillary ligands is more prevalent than other species to form high-nuclearity lanthanide clusters with well-defined structure through ligand-controlled hydrolysis of the lanthanide ions.[12a]

IR Characterizations. A comparison of the IR spectra of the complexes with the ligands provides evidence for the coordination mode of the ligands (Figure S3, Supporting Information); the relevant characteristic bands of ligands and complexes are given in Table 1. The broad absorptions in the 3100−3650 cm^{-1} region for the complexes can be assigned to the stretching of —OH. The absence of absorption in the ν(O—H) region of the free ligands is considered as evidence that there exists a strong intramolecular hydrogen bond between —OH and C═O groups, which considerably weakens and broadens the ν(O—H) vibration. The relatively strong ν(C═O) vibrations at 1601−1620 cm^{-1} in these complexes are appreciably red-shifted by a range of 14−29 cm^{-1} relative to that of the free ligands, indicating the coordination of C═O groups with Eu^{3+} ions. The stretching frequencies of Ph—O vibrations of the complexes (1240−1254 cm^{-1}) are also red-shifted relative to the free ligands. The comparison of the IR spectra obtained for the six complexes exhibits a similar feature in the 4000−400 cm^{-1} region, which indicates the similar structural features of these complexes.

Electronic Absorption Spectra. The UV−vis absorption spectra of the free ligands (HL1−HL6) and the corresponding nonanuclear europium clusters (Eu9-1 to Eu9-6) were recorded in acetonitrile solutions (2.0×10^{-5} mol/cm^3) at room temperature (for nonanuclear clusters, the concentrations of the solutions were based on Eu(III) ion). Considering that the nonanuclear cluster might dissociate into smaller species such as $EuL_2(OH)(H_2O)_2$ and $EuL_3(H_2O)_2$ in the dilute acetonitrile solution, we measure the absorption spectra for both the mononuclear europium complexes ($EuL_3(H_2O)_2$: Eu-1 to Eu-6) and nonanuclear clusters (Eu9-1 to Eu9-6) in either solid state or acetonitrile solution (Figures S4 and S5, Supporting Information). The results show that there is no obvious difference between the absorption spectra of monomers and clusters under both conditions, indicating that the coordinated ligands in monomers and clusters are under identical influence of the Eu(III) ion. As shown in Figure 2, the absorption bands

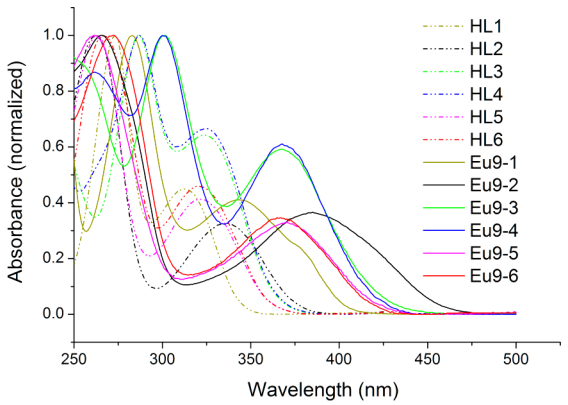

Figure 2. UV−vis absorption spectra of the ligands and the corresponding europium clusters in acetonitrile solution ($c = 2.0 \times 10^{-5}$ mol·cm^{-3}). The concentrations of the clusters were based on Eu(III) ion. All spectra are normalized to a constant intensity at the maximum.

located in the region 250−290 nm are primarily attributed to the π−π^* electronic transitions of the ligands. The lower energy transitions are associated with the shift of electron density from the phenolate oxygen to the π^* orbitals of the aromatic rings with maxima at 300−350 nm. The molar absorption coefficient values of the ligands, calculated at the absorption maxima of the lower energy bands (λ_{max}), illustrate good light absorption ability of the ligands (Table 2). The introduction of a fluorine or methoxy group in the 4-position of the HL2 ligand moderately shifts the lower energy absorption bands toward the blue region. Furthermore, due to the reduced π-conjugation, the ligand HL1 displays a more apparent blue shift with the lower energy absorption band at 290−340 nm (λ_{max} = 313 nm). Upon complexation with Eu(III) ions, as expected, the absorption profiles are dominated by the ligands and the lower energetic transitions are significantly red-shifted about 2879−3978 cm^{-1}. Interestingly, the lower energy absorption bands of these complexes extend to the visible region, rendering the corresponding europium clusters the

Table 1. The Relevant Characteristic IR Bands (cm^{-1}) of the Ligands and the Complexes

	Eu9-1/HL1	Eu9-2/HL2	Eu9-3/HL3	Eu9-4/HL4	Eu9-5/HL5	Eu9-6/HL6
ν(—OH)	3449/-	3356/-	3334/-	3332/-	3420/-	3396/-
ν(C═O)	1601/1622	1611/1627	1607/1629	1604/1633	1620/1634	1619/1634
ν(Ph—O)	1243/1255	1240/1244	1247/1259	1247/1257	1254/1258	1252/1258

dx.doi.org/10.1021/ic401191e | Inorg. Chem. XXXX, XXX, XXX−XXX

Table 2. The Absorption Maxima of the Lower Energy Bands (λ_{max}) and the Related Molar Absorption Coefficient Values (ε) for the Ligands and Europium Clusters

	HL1	HL2	HL3	HL4	HL5	HL6
$\varepsilon/10^4$ L mol^{-1} cm^{-1} (λ_{max}/nm)	0.64 (313)	0.35 (338)	1.14 (324)	1.26 (324)	0.53 (321)	0.63 (320)
	Eu9-1	Eu9-2	Eu9-3	Eu9-4	Eu9-5	Eu9-6
$\varepsilon^a/10^4$ L mol^{-1} cm^{-1} (λ_{max}/nm)	1.09 (344)	0.63 (385)	1.96 (369)	2.23 (368)	0.93 (368)	1.12 (366)
$\Delta E(\lambda_{max})^b$/cm^{-1}	2879	3612	3764	3690	3978	3927

[a]The concentrations of the clusters in acetonitrile were based on Eu(III) ion. [b]The differences in absorption maxima of the lower energy bands in energy units (cm^{-1}).

potential property of being long wave sensitized luminescent materials.[18]

Photoluminescence Properties. The solid-state excitation spectra of complexes (Eu9-1 to Eu9-6) are recorded at room temperature. As shown in Figure S6 in the Supporting Information, the excitation spectra of complexes (Eu9-2 to Eu9-6), obtained by monitoring the $^5D_0 \rightarrow {}^7F_2$ transition of Eu(III) ion at 614 nm, are very similar. They all feature strong bands in the range 350−450 nm with the maximal absorptions around 405 nm. The excitation spectrum of complex Eu9-1 shows a maximal absorption around 372 nm owing to the reduced conjugated system of HL1; furthermore, the narrow band at 464 nm corresponding to the $^7F_0 \rightarrow {}^5D_2$ hypersensitive transition of Eu(III) ion can also be clearly observed. The excitation spectra overlap well with the absorption spectra of the europium clusters, evidencing that the emissions arise from the antenna effects of the ligands.[19]

The europium clusters exhibit the characteristic Eu(III) emissions when excited at 372 nm for Eu9-1 and 405 nm for the others at both ambient and low temperatures, indicating efficient energy transfer from the ligands to the Eu(III) center. Due to the similar coordination environment around the Eu(III) center, crystal field splittings of the ^7F_J levels (J = 0−4) extracted from emission spectra (77 K) are identical. Several features can be outlined from the analysis of the luminescence spectrum of the representative cluster Eu9-3 at 77 K (Figure S7, Supporting Information). The well resolved five sharp peaks at 578, 590, 614, 652, and 700 nm correspond to the transitions from the $^5D_0$ excited state to the ^7F_J (J = 0; 1; 2; 3; 4) ground state multiplet.[20] It is well-known that the $^5D_0 \rightarrow {}^7F_1$ magnetic dipole transition at 590 nm is independent of the coordination sphere, while the electric dipole transition $^5D_0 \rightarrow {}^7F_2$ at 614 nm is extremely sensitive to the nature and symmetry of the coordinating environment, which can be further enhanced by the distortion of the symmetry around the europium ion.[21] Thus, the domination of the electric dipole $^5D_0 \rightarrow {}^7F_2$ transition at 614 nm indicates the presence of a low-symmetry Eu(III) site, which is confirmed by the crystal structure. The singlet of the $^5D_0 \rightarrow {}^7F_0$ transition at about 578 nm indicates the presence of only single site symmetry of Eu^{3+} ion corresponding to the basal Eu(III) in the nonanuclear cluster, because the $^5D_0 \rightarrow {}^7F_0$ transition is strictly forbidden (by the electric and magnetic dipole mechanisms) for the highly symmetrical coordination around the central Eu(III) ion.[12a]

Notably, although the emission spectra of the clusters at 298 K have analogical profiles because of their similar structures, the luminescence efficiencies of the complexes with different chelating ligands decrease in the sequence of Eu9-6 > Eu9-5 > Eu9-4 > Eu9-3 > Eu9-2 > Eu9-1 (Figure 3). Within a general paradigm, the overall luminescence quantum yield of the europium complex upon excitation of the chromophore is determined by the sensitization efficiency of the ligand (η_{sens})

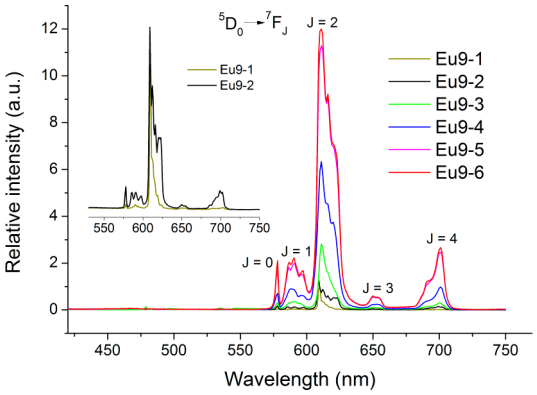

Figure 3. Emission spectra of clusters Eu9-1 to Eu9-6 at 298 K in the solid state (λ_{ex} = 372 for Eu9-1 and 405 nm for the others).

and by the intrinsic quantum yields (Φ_{Eu}) (eq 1).[22] The intrinsic quantum yield of the luminescent europium complex (Φ_{Eu}) can be evaluated from eqs 2 and 3,[23] where τ_{obs}/τ_{rad} are the observed and radiative lifetimes of Eu($^5D_0$), $A_{MD,0}$ is the spontaneous emission probability for the $^5D_0 \rightarrow {}^7F_1$ transition in vacuo (14.65 s^{-1}), I_{tot}/I_{MD} is the ratio of the total integrated $^5D_0 \rightarrow {}^7F_J$ emissions (J = 0−4) to the magnetic dipole $^5D_0 \rightarrow {}^7F_1$ transition, and the refractive index of the medium (n) is taken to be equal to 1.5 in the solid sample that is commonly encountered for coordination complexes.

$$\Phi_{tot} = \eta_{sens} \times \Phi_{Eu} \quad (1)$$

$$\Phi_{Eu} = \tau_{obs}/\tau_{rad} \quad (2)$$

$$1/\tau_{rad} = A_{MD,0} \times n^3 \times (I_{tot}/I_{MD}) \quad (3)$$

Table 3 summarizes the Φ_{tot}, τ_{obs}, and other photophysical parameters. The presence of O−H oscillators may be a key factor causing the small luminescence quantum yields and

Table 3. Radiative Lifetimes (τ_{rad}), Luminescence Lifetimes (τ_{obs}), Sensitization Efficiencies (η_{sens}), Intrinsic Quantum Yields (Φ_{Eu}), and Overall Quantum Yields (Φ_{tot}) for the Clusters Eu9-1 to Eu9-6 at 298 K in Solid State

complexes	τ_{rad} (ms)	τ_{obs} (ms)	η_{sens} (%)	Φ_{Eu} (%)	$\Phi_{tot}{}^a$ (%)
Eu9-1	2.58	0.51		19.8	<0.5
Eu9-2	2.59	0.30		11.6	<0.5
Eu9-3	2.60	0.33	11.8	12.7	1.5
Eu9-4	2.61	0.38	26.0	14.6	3.8
Eu9-5	2.62	0.46	40.9	17.6	7.2
Eu9-6	2.61	0.48	45.7	18.4	8.4

[a]Φ_{tot} was measured using an integrating sphere method with integrated emission ranging from 550 to 750 nm.

dx.doi.org/10.1021/ic401191e | Inorg. Chem. XXXX, XXX, XXX−XXX

Table 4. The Lowest Singlet and Triplet Energy Levels of the Ligands in the Gadolinium Complexes

	HL1	HL2	HL3	HL4	HL5	HL6
$E(S_1)$, cm^{-1}	24694	21834	23310	23529	23786	23809
$E(T_1)$, cm^{-1}	23094	17761	17921	18181	18416	18498
$\Delta E(T_1-{}^5D_0)$, cm^{-1}	5794	461	621	881	1116	1198

lifetimes.[24] It is worth noting that the radiative lifetimes (τ_{rad}) of the complexes are similar to each other, resulting in comparable intrinsic quantum yields (Φ_{Eu}) within the range 11.6−19.8%. The results imply that the luminescence efficiencies of the complexes mainly depend on the energy transfer efficiencies between the ligands and the Eu(III) ions.

Energy Transfer between Ligands and Eu^{3+}. The most well documented mechanism for the energy transfer from a chromophore ligand to europium ion involves the intersystem crossing (ISC) from the first excited singlet state of the ligand to the lowest triplet state, which then transfers energy to the europium-emitting resonance level.[25] Accordingly, we have determined the relevant ligand-centered electronic states in the complexes. On account of the difficulty in observing the singlet state by fluorescent emissions of the corresponding non-emissive Ln complex (Gd, La, Lu) at room temperature, the energy levels of S_1 are estimated with a reported method by referring to the UV−vis absorption edges of the corresponding mononuclear gadolinium complexes ($GdL_3(H_2O)_2$ shortened as Gd-1 to Gd-6) (Figure S8, Supporting Information).[26] Since the lowest-lying excited level of the Gd(III) ion ($^6P_{7/2}$, at 32150 cm^{-1}) is too high to permit any energy transfer from the ligand to the metal center, the phosphorescence spectra of the Gd^{3+} complexes can reveal the lowest triplet energy levels of the ligands.[27] The triplet energy levels of the ligands are determined by the phosphorescence spectra of the gadolinium complexes ($Gd(L)_3(H_2O)_2$) at 77 K (Figure S9, Supporting Information). For comparison, the singlet and triplet state energy levels are summarized in Table 4. The results show that the energy differences between singlet and triplet states for HL_3−HL_6, $\Delta E(^1\pi\pi^*-{}^3\pi\pi^*)$, are larger than 5000 cm^{-1}, while those of HL_1 and HL_2 only amount to 1600 and 4073 cm^{-1}, respectively. According to Reinhoudt's empirical rule, the intersystem crossing process becomes effective when $\Delta E(^1\pi\pi^*-{}^3\pi\pi^*)$ is at least 5000 cm^{-1}.[28] Thus, the intersystem crossing processes of ligands (HL3−HL6) are efficient, which render these ligands the potential ability to transfer energy to europium ion efficiently.

It is well-known that a suitable energy gap between the triplet energy level of the ligand (T_1) and the radiation state of the Eu^{3+} ion ($^5D_0$) is required for an optimal ligand-to-europium energy transfer process.[29] As shown in Table 4, the energy gap $\Delta E(T_1 \rightarrow {}^5D_0)$ of 5794 cm^{-1} for HL1 is obviously too high to allow an effective energy transfer, resulting in a poor sensitization efficiency of the ligand. As already shown by Crosby et al., the triplet state of the HL_2 ligand (17761 cm^{-1}) is critically close to the $^5D_0$ emitting state,[13e] which can lead to the thermally assisted back-energy transfer from the europium $^5D_0$ state to the triplet state of the ligand (BET) and a very low luminescence efficiency of Eu9-2. Interestingly, the introduction of substituents on the ligand (HL_2) apparently raises the lowest triplet states of the ligands with the trend HL3 < HL4 < HL5 < HL6, lying between the $^5D_1$ (19 070 cm^{-1}) and $^5D_0$ (17 300 cm^{-1}) excited states of the europium ion.[30] As shown in Table 3, the ligand sensitization efficiencies (η_{sens}) increase obviously with the trend Eu9-2 < Eu9-3 < Eu9-4 < Eu9-6 < Eu9-5, following the increasing order of the triplet state energy levels of the corresponding ligands. This result implies that the triplet energy levels of this kind of ligands can be fine-tuned by the substituents on the ligands, leading to a more energetically compatible, efficient energy transfer process to the $^5D_0$ emitting level of Eu^{3+}.

Computational Studies. It is known that the optoelectronic properties depend mainly on the frontier molecular orbitals (FMOs), especially the highest occupied molecular orbital (HOMO, H) and the lowest unoccupied molecular orbital (LUMO, L).[31] In this subsection, comprehensive density functional theory (DFT) calculations using the B3LYP functional have been performed on the free ligands to ascertain the effects of the substituents involved in tuning electronic features of the ligands. Moreover, as a simplified model, the corresponding mononuclear europium complexes ($Eu(L)_3(H_2O)_2$) are calculated at the B3LYP/6-311G++(d,p)//SDD (Eu) level to analyze the influence of the Eu(III) ion. The optimized geometrical structures of the ligands and complexes are depicted in Figure S10 (Supporting Information). There are two conformations for ligands HL3 and HL4 due to the less coexistent orientations of methoxy groups in the clusters (named HL3′ and HL4′). The HOMO and LUMO distribution, energy levels, and energy gaps of the ligands and mononuclear europium complexes are shown in Figure 4 and Table S10 (Supporting Information), respectively.

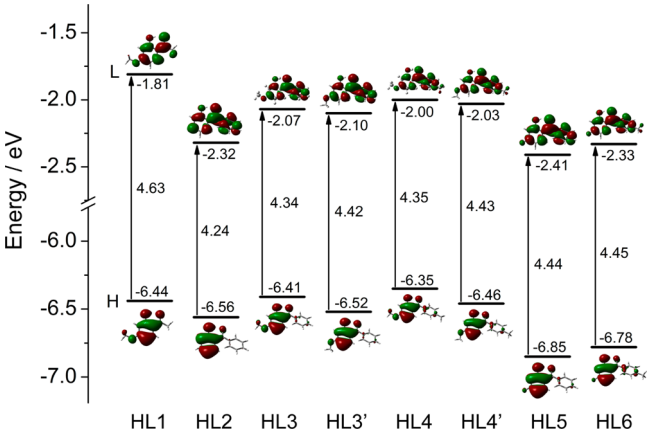

Figure 4. Presentation of the energy levels, energy gaps, and orbital composition distribution of the HOMO and LUMO for the ligands.

Orbital analyses of the compositions of the HOMOs and LUMOs for HL1−HL6 show that the HOMOs are mainly located at phenolate moieties of the ligands while the LUMOs extend to the whole molecules (Figure 4).[32] The HOMO energy of HL1 is similar to those of HL3 and HL4, due to the similar HOMOs. The energy of the LUMO, however, is considerably higher owing to the reduced π-conjugation and thus resulting in a larger HOMO−LUMO energy gap (HLG) for HL1 (4.63 eV) compared with that of the other ligands. On the contrary, the HLG of the parent ligand HL2 is the smallest (4.24 eV) due to the contribution of the phenyl π-orbital. It is

dx.doi.org/10.1021/ic401191e | Inorg. Chem. XXXX, XXX, XXX−XXX

interesting to note that the HOMO and LUMO energies of the ligands depend to a large extent on the nature of the substituents. Similar to the observation for tris(8-hydroxyquinolinato) aluminum (Alq_3), a methoxy substitution at the 4-position of the phenolate ring raises both the HOMO and LUMO levels due to its electron-donating property, whereas the fluorine atom mainly exhibits a strong electron-withdrawing effect to lower the energy levels.[33] Since 4-OMe particularly affects the LUMO level, while 4-fluorine atom influences the HOMO level significantly, the energy gaps of HL3 and HL5 are larger than that of parent ligand HL2. Moreover, the attachment of an extra electron-donating methyl groups in HL4 and HL6 led to a slight effect on the orbital energies with the HLGs raised by 0.01 eV compared with HL3 and HL5, respectively. As a result, the HLGs increase in the sequence of HL2 < HL3 < HL4 < HL5 < HL6 < HL1, which is in agreement with the excited state levels of these ligands.

As expected, europium complexes gave smaller HOMO−LUMO energy gaps due to the combination of three ligands and one trivalent europium ion (Table S10, Supporting Information). We found that the HOMOs for the complexes are mainly based on two phenolate moieties, while the LUMOs are localized on two entire ligands. Moreover, population analysis revealed that the contributions of the europium ions to HOMO and LUMO are negligible (less than 5%) except for Eu-1, of which the Eu(III) ions account for 22.10% of the LUMO. The results interpret very weak metal−ligand mixing in the HOMOs and LUMOs. The calculated data suggests that the substituents affect the frontier molecular orbitals of these complexes apparently, which is similar to that observed in the corresponding ligands. Thus, the HLG increases in the order Eu-2 < Eu-3 < Eu-4 < Eu-5 < Eu-6 < Eu-1. On the basis of the discussion, it is reasonable to conclude that the optical properties of these clusters are dependent on the electronic features of the ligands, which can be fine-tuned by the substituents in the ligands.

CONCLUSIONS

In summary, six novel diabolo-shaped nonanuclear Eu(III) clusters with appealing structures and interesting optical properties have been synthesized with modified 2-hydroxybenzophenone as supporting ligands. X-ray diffraction analysis reveals that the compounds are all nonanuclear clusters with a similar core $[Eu(III)_9(L)_{16}(\mu_3\text{-}OH)_8(\mu_4\text{-}O)(\mu_4\text{-}OH)]$, which comprises two vertex-sharing square pyramids arranged in a "staggered" fashion. The photophysical studies show that all the complexes exhibit characteristic red luminescence of Eu^{3+} under long-wavelength excitation with the luminescent efficiencies decreasing in the sequence Eu9-6 > Eu9-5 > Eu9-4 > Eu9-3 > Eu9-2 > Eu9-1. The phenomena are rationalized by the studies on the lowest electronic excited states of these ligands. The supporting DFT computational results confirm that the excited energy levels of these ligands can be fine-tuned by incorporating substitutions into the ligands. The introduction of fluorine or methoxy substituents on the ligand, especially for the fluorine, can apparently raise the lowest triplet states of the ligands to the values facilitating efficient energy transfer process to the $^5D_0$ emitting level of Eu^{3+}, which result in more efficient luminescence. Taken collectively, manipulation of the electronic features of the 2-hydroxybenzophenone by substituents is a viable strategy for obtaining new luminescent europium clusters. The specific design of polynuclear complexes with interesting optical properties is now under way.

EXPERIMENTAL SECTION

Materials. Diethyl ether and triethylamine (TEA) were dried using standard procedures. All the other reagents were used as received from commercial sources, unless otherwise stated.

Physical Measurements. ^1H and ^{13}C NMR spectra were obtained using a Bruker DPX-400 MHz spectrometer in $CDCl_3$. The following standard abbreviations are used for characterization of NMR signals: s, singlet; d, doublet; t, triplet; m, multiplet; dd, doublet of doublets. HRMS were determined on a Waters Q-Tof Micro MS/MS System ESI spectrometer. Elemental analysis for C, H, and N was carried out with a Carlo-Erba1106 Elemental Analyzer. IR spectra were performed on a Perkin-Elmer FTIR GX instrument using KBr pellets in the 400−4000 cm^{-1} region. Absorption spectra were measured on a Perkin-Elmer Lambda 900 spectrometer at room temperature. The excitation and emission spectra of the Eu(III) complexes in solid state at room temperature (298 K) were recorded at an angle of 22.5° (front face) on a HORIBA JOBIN YVON FluoroMax-P spectrophotometer equipped with both continuous and pulsed xenon lamps, and the emission spectra at 77 K of the clusters and mononuclear gadolinium complexes were recorded by cooling the sample with liquid nitrogen in a Dewar flask. The observed luminescence lifetimes of the europium clusters were determined under excitation maximum and monitoring the $^5D_0-{}^7F_2$ with a HORIBA JOBIN YVON FluoroMax-P spectrophotometer. The emission (550−750 nm) quantum yields of the clusters were obtained with a SPEX Fluorolog spectrofluorimeter at room temperature using an integrating sphere method.[34] Three measurements were carried out for each sample. The errors in the quantum yield values associated with this technique were estimated within ±10%.[35]

X-ray Crystallography. Crystal diffraction data for the complexes Eu9-1, Eu9-3, Eu9-4, and Eu9-6 were collected on an Oxford Diffraction Xcalibur CCD diffractometer with graphite-monochromatized Mo Kα radiation (λ = 0.71073 Å) at room temperature using the ω-scan technique. The program CrysAlisPro was employed for data collection and data reduction.[36] The structures were solved by direct methods, and the non-hydrogen atoms were refined anisotropically by a full-matrix least-squares method on F^2 using the SHELXTL-97 program.[37] Part of the MeO groups of the HL4 are refined to be disordered over two possible sites with site occupancy factors of 0.52:0.48. Moreover, in order to keep the global neutrality, we imposed a disorder on the occupancy of the hydrogen atom supported by the μ_4-O groups (μ_4-(O, OH) 50:50). Similar phenomena were also previously reported.[12a] The hydrogen atoms were included in the structure factor calculation at ideal positions using a riding model. Complete crystal structure results of the complexes as CIF files including bond lengths, angles, and atomic coordinates are available as Supporting Information.

Computational Methodology. The ground-state geometries of the ligands were optimized with density functional theory (DFT) using Becke's three-parameter hybrid exchange functional combined with Lee−Yang−Parr's correlation functional (B3LYP).[38] Stuttgart-Dresden effective core potential (designed as SDD ECP) basis sets[39] were used for the Eu(III) ion, while the 6-311G++(d,p) basis set was employed for all other atoms. All calculations were done in the gas phase with the Gaussian 09 package.[40] Vibrational frequencies were calculated at the same theoretical level to confirm that each configuration was a minimum on the potential energy surface. Graphic representations for optimized geometrical structures and molecular orbitals for the ground state were obtained with GaussView.

Syntheses. The methanol solutions of $LnCl_3{\cdot}xH_2O$ (0.1 mol/L) were prepared from their oxides using a modified version of a previously published procedure.[41] The europium complexes $(EuL_3(H_2O)_2$: Eu-1 to Eu-6) are synthesized according to the literature procedure.[13a,b]

Synthesis of (4-Fluoro-2-hydroxyphenyl)phenylmethadone (HL5). Benzoyl chloride (2.81 g, 20.0 mmol) was added slowly to a diethyl ether solution (50 mL) of 3-fluorophenol (2.00 g, 17.8 mmol) and triethylamine (2.02 g, 20.0 mmol) under a nitrogen atmosphere. The mixture was refluxed for about 1 h under stirring. Then, the

dx.doi.org/10.1021/ic401191e | Inorg. Chem. XXXX, XXX, XXX−XXX

reaction was quenched with water (~10 mL) and the pH of the solution was adjusted to 5 with 10 wt % NaOH solution. The solution was extracted with ethyl acetate (3 × 50 mL), and the organic phase was then dried ($MgSO_4$), evaporated, and concentrated to dryness under reduced pressure. The resulting crude product was mixed with $AlCl_3$ (2.53 g, 19.0 mmol) under a nitrogen atmosphere, and the resultant mixture was heated for 30 min at 200 °C. After cooling to room temperature, the solid was slowly added to ice-cooled 10% HCl solution under stirring. The final product was then obtained through column chromatography with a moderate yield of 79% (3.04 g). ^{1}H NMR (400 MHz, $CDCl_3$) δ 12.43 (d, 1H), 7.62 (m, 4H), 7.52 (m, 2H), 6.76 (dd, 1H), 6.60 (m, 1H). ^{13}C NMR (100 MHz, $CDCl_3$) δ 200.6, 167.5 (d), 165.8 (d), 137.8, 136.0 (d), 132.1, 129.0, 128.5, 116.2 (d), 107.0 (d), 105.1 (d). Anal. Calcd for $C_{13}H_9FO_2$ (%): C, 72.22; H, 4.20. Found (%): C, 72.20; H, 4.19. HRMS (ESI) calcd for $C_{13}H_{10}FO_2$ $[M + H]^+$: 217.0665, found 217.0663.

Synthesis of (4-Fluoro-2-hydroxyphenyl)-(4-methylphenyl)-methadone (HL6). This compound was prepared by using the method described for the synthesis of HL5. Yield 72% (2.95 g). ^{1}H NMR (400 MHz, $CDCl_3$) δ 12.45 (d, 1H), 7.63 (dd, 1H), 7.56 (d, 2H), 7.31 (d, 2H), 6.74 (m, 1H), 6.58 (m, 1H), 2.45 (s, 3H). ^{13}C NMR (100 MHz, $CDCl_3$) δ 200.3, 167.3 (d), 165.7 (d), 142.9, 135.9 (d), 135.0, 129.3, 129.1, 116.3 (d), 106.8 (d), 105.0 (d), 21.6. Anal. Calcd for $C_{14}H_{11}FO_2$ (%): C, 73.03; H, 4.82. Found (%): C, 73.00; H, 4.79. HRMS (ESI) calcd for $C_{14}H_{12}FO_2$ $[M + H]^+$: 231.0821, found 231.0826.

Synthesis of Mononuclear Gadolinium Complexes $Gd(L)_3(H_2O)_2$. The ligand HL (3 mmol) and $GdCl_3{\cdot}xH_2O$ (1.00 mol) were dissolved in 30 mL of ethanol, and then, the pH of the mixture was adjusted to 7 with 20 wt % NaOH aqueous solution. The resultant solution was heated and stirred at 60 °C for 3 h, and then cooled to room temperature. The precipitates were filtered and purified by recrystallization from an ethanol–water mixed solution, dried in air, and then dried in a vacuum.

Gd-1 ($GdC_{27}H_{25}O_{11}$). Yield: 63%. Anal. Calcd (%): C, 47.50; H, 3.69. Found: C, 47.45; H, 3.63.

Gd-2 ($GdC_{39}H_{25}O_8$). Yield: 82%. Anal. Calcd (%): C, 60.14; H, 3.24. Found: C, 60.18; H, 3.19.

Gd-3 ($GdC_{42}H_{31}O_{11}$). Yield: 70%. Anal. Calcd (%): C, 58.05; H, 3.60. Found: C, 57.93; H, 3.54.

Gd-4 ($GdC_{45}H_{37}O_{11}$). Yield: 72%. Anal. Calcd (%): C, 59.33; H, 4.09. Found: C, 59.38; H, 4.02.

Gd-5 ($GdC_{39}H_{22}F_3O_8$). Yield: 65%. Anal. Calcd (%): C, 56.24; H, 2.66. Found: C, 56.22; H, 2.61.

Gd-6 ($GdC_{42}H_{28}F_3O_8$). Yield: 69%. Anal. Calcd (%): C, 57.66; H, 3.23. Found: C, 57.61; H, 3.18.

Synthesis of Clusters: General Procedure. A 1 mmol portion of $EuCl_3{\cdot}xH_2O$ and 2 mmol of HL were dissolved in 10 mL of methanol. After stirring for 15 min, 4 mmol of triethylamine was added dropwise to the solution, and then, the mixture was stirred for 3 h at room temperature. The resultant solution was left unperturbed to allow the slow evaporation of the solvent. Yellow block single crystals, suitable for X-ray diffraction analysis, were formed after 5 days. Yields: 29–43% based on Eu.

$[Eu(III)_9(L1)_{16}(\mu_3\text{-}OH)_8(\mu_4\text{-}O)(\mu_4\text{-}OH)]{\cdot}2H_2O{\cdot}2CH_3OH$ (Eu9-1, yield: 36%): Anal. Calcd for $Eu_9C_{146}H_{165}O_{62}$ (%): C, 40.98; H, 3.89. Found (%): C, 40.86; H, 3.81. IR (KBr, cm^{-1}): 3449 (m), 1601 (s), 1517(s), 1371 (s), 1243 (s), 1138 (m), 1063 (m), 983 (m), 848 (m), 788 (w), 572 (w).

$[Eu(III)_9(L2)_{16}(\mu_3\text{-}OH)_8(\mu_4\text{-}O)(\mu_4\text{-}OH)]$ (Eu9-2, yield: 31%): Anal. Calcd for $Eu_9C_{208}H_{153}O_{42}$ (%): C, 53.24; H, 3.29. Found (%): C, 53.19; H, 3.22. IR (KBr, cm^{-1}): 3356 (w), 3057 (w), 1611(s), 1332 (m), 1240 (s), 1148 (m), 941 (w), 760 (m), 701 (m).

$[Eu(III)_9(L3)_{16}(\mu_3\text{-}OH)_8(\mu_4\text{-}O)(\mu_4\text{-}OH)]$ (Eu9-3, yield: 43%): Anal. Calcd for $Eu_9C_{224}H_{185}O_{58}$ (%): C, 52.01; H, 3.61. Found (%): C, 51.98; H, 3.52. IR (KBr, cm^{-1}): 3334 (w), 1607 (s), 1517(s), 1358 (m), 1247 (s), 1114 (m), 1029 (w), 841 (w), 702 (m), 599 (w).

$[Eu(III)_9(L4)_{16}(\mu_3\text{-}OH)_8(\mu_4\text{-}O)(\mu_4\text{-}OH)]$ (Eu9-4, yield: 41%): Anal. Calcd for $Eu_9C_{240}H_{217}O_{58}$ (%): C, 53.41; H, 4.05. Found (%): C, 53.35; H, 3.91. IR (KBr, cm^{-1}): 3332 (w), 1604 (s), 1516 (s), 1364 (s), 1247 (s), 1113 (m), 1030 (w), 836 (m), 764 (m), 584 (w).

$[Eu(III)_9(L5)_{16}(\mu_3\text{-}OH)_8(\mu_4\text{-}O)(\mu_4\text{-}OH)]$ (Eu9-5, yield: 32%): Anal. Calcd for $Eu_9C_{208}H_{137}F_{16}O_{42}$ (%): C, 50.17; H, 2.77. Found (%): C, 50.10; H, 2.69. IR (KBr, cm^{-1}): 3420 (m), 1621 (s), 1532 (s), 1418 (s), 1254 (s), 990 (m), 853 (m), 758 (m), 579 (m).

$[Eu(III)_9(L6)_{16}(\mu_3\text{-}OH)_8(\mu_4\text{-}O)(\mu_4\text{-}OH)]$ (Eu9-6, yield: 29%): Anal. Calcd for $Eu_9C_{224}H_{169}F_{16}O_{42}$ (%): C, 51.70; H, 3.27. Found (%): C, 51.65; H, 3.21. IR (KBr, cm^{-1}): 3396 (m), 1619 (s), 1532 (s), 1417 (s), 1252 (s), 990 (w), 701 (m).

■ ASSOCIATED CONTENT

Ⓢ Supporting Information

X-ray crystallographic data of Eu9-1, Eu9-3, Eu9-4, and Eu9-6 in CIF format. Crystal data and structure refinement parameters for clusters, thermal ellipsoid plot of the clusters, selected bond lengths and angles for Eu9-3, IR spectra for the ligands and clusters, absorption spectra of the mononuclear europium complexes (Eu-1 to Eu-6) and nonanuclear europium clusters (Eu9-1 to Eu9-6) in solid state and in acetonitrile at room temperature, excitation spectra of clusters Eu9-1 to Eu9-6 at 298 K, luminescence spectrum of the cluster Eu9-3 at 77 K in the solid state, UV–vis absorption spectra of the mononuclear gadolinium complexes, phosphorescence spectra of the mononuclear gadolinium complexes $(Gd(L)_3(H_2O)_2)$ at 77 K, optimized ground-state structures of the ligands and mononuclear europium complexes (Eu-1 to Eu-6) together with Cartesian coordinates, the HOMO and LUMO distribution, and energy levels and energy gaps of the mononuclear europium complexes. This material is available free of charge via the Internet at http://pubs.acs.org.

■ AUTHOR INFORMATION

Corresponding Authors

*E-mail: dcx@zzu.edu.cn

*E-mail: mpsong@zzu.edu.cn.

Notes

The authors declare no competing financial interest.

■ ACKNOWLEDGMENTS

This work was supported by the Specialized Research Fund for the Doctoral Program of Higher Education (20114101130002) and the National Natural Science Foundation of China (21071128).

■ REFERENCES

(1) (a) Andrews, P. C.; Gee, W. J.; Junk, P. C.; Massi, M. *New J. Chem.* **2013**, *37*, 35–48. (b) Canaj, A. B.; Tzimopoulos, D. I.; Philippidis, A.; Kostakis, G. E.; Milios, C. J. *Inorg. Chem.* **2012**, *51*, 7451–7453. (c) Feng, W.; Zhang, Y.; Zhang, Z.; Lü, X.; Liu, H.; Shi, G.; Zou, D.; Song, J.; Fan, D.; Wong, W.-K.; Jones, R. A. *Inorg. Chem.* **2012**, *51*, 11377–11386. (d) Bozoklu, G.; Gateau, C.; Imbert, D.; Pécaut, J.; Robeyns, K.; Filinchuk, Y.; Memon, F.; Muller, G.; Mazzanti, M. *J. Am. Chem. Soc.* **2012**, *134*, 8372–8375. (e) Li, X.-L.; He, L.-F.; Feng, X.-L.; Song, Y.; Hu, M.; Han, L.-F.; Zheng, X.-J.; Zhang, Z.-H.; Fang, S.-M. *CrystEngComm* **2011**, *13*, 3643–3645. (f) Andrews, P. C.; Beck, T.; Forsyth, C. M.; Fraser, B. H.; Junk, P. C.; Massi, M.; Roesky, P. W. *Dalton. Trans.* **2007**, 5651–5654. (g) Gee, W. J.; Hierold, J.; MacLellan, J. G.; Andrews, P. C.; Lupton, D. W.; Junk, P. C. *Eur. J. Inorg. Chem.* **2011**, *2011*, 3755–3760.

(2) (a) Xu, X.; Zhao, L.; Xu, G.-F.; Guo, Y.-N.; Tang, J.; Liu, Z. *Dalton. Trans.* **2011**, *40*, 6440–6444. (b) Luzon, J.; Sessoli, R. *Dalton. Trans.* **2012**, *41*, 13556–13567. (c) Jami, A. K.; Baskar, V.; Sañudo, E. C. *Inorg. Chem.* **2013**, *52*, 2432–2438.

(3) (a) Hauser, C. P.; Thielemann, D. T.; Adlung, M.; Wickleder, C.; Roesky, P. W.; Weiss, C. K.; Landfester, K. *Macromol. Chem. Phys.* **2011**, *212*, 286−296. (b) Andrews, P. C.; Brown, D. H.; Fraser, B. H.; Gorham, N. T.; Junk, P. C.; Massi, M.; St Pierre, T. G.; Skelton, B. W.; Woodward, R. C. *Dalton. Trans.* **2010**, *39*, 11227−11234.
(4) (a) Cheng, J.-W.; Zhang, J.; Zheng, S.-T.; Zhang, M.-B.; Yang, G.-Y. *Angew. Chem., Int. Ed.* **2006**, *45*, 73−77. (b) Zheng, Z. *Chem. Commun.* **2001**, 2521−2529. (c) Feng, W.; Zhang, Y.; Lu, X.; Hui, Y.; Shi, G.; Zou, D.; Song, J.; Fan, D.; Wong, W.-K.; Jones, R. A. *CrystEngComm* **2012**, *14*, 3456−3463.
(5) (a) Wu, Y.; Morton, S.; Kong, X.; Nichol, G. S.; Zheng, Z. *Dalton. Trans.* **2011**, *40*, 1041−1046. (b) Tong, Y.-Z.; Wang, Q.-L.; Yang, G.; Yang, G.-M.; Yan, S.-P.; Liao, D.-Z.; Cheng, P. *CrystEngComm* **2010**, *12*, 543−548. (c) Andrews, P. C.; Deacon, G. B.; Frank, R.; Fraser, B. H.; Junk, P. C.; MacLellan, J. G.; Massi, M.; Moubaraki, B.; Murray, K. S.; Silberstein, M. *Eur. J. Inorg. Chem.* **2009**, *2009*, 744−751. (d) Andrews, P. C.; Beck, T.; Fraser, B. H.; Junk, P. C.; Massi, M.; Moubaraki, B.; Murray, K. S.; Silberstein, M. *Polyhedron* **2009**, *28*, 2123−2130. (e) Andrews, P. C.; Gee, W. J.; Junk, P. C.; MacLellan, J. G. *Polyhedron* **2011**, *30*, 2837−2842.
(6) (a) Alexandropoulos, D. I.; Mukherjee, S.; Papatriantafyllopoulou, C.; Raptopoulou, C. P.; Psycharis, V.; Bekiari, V.; Christou, G.; Stamatatos, T. C. *Inorg. Chem.* **2011**, *50*, 11276−11278. (b) Andrews, P. C.; Gee, W. J.; Junk, P. C.; MacLellan, J. G. *Inorg. Chem.* **2010**, *49*, 5016−5024. (c) Yan, P.-F.; Lin, P.-H.; Habib, F.; Aharen, T.; Murugesu, M.; Deng, Z.-P.; Li, G.-M.; Sun, W.-B. *Inorg. Chem.* **2011**, *50*, 7059−7065.
(7) (a) Kong, X.-J.; Long, L.-S.; Zheng, L.-S.; Wang, R.; Zheng, Z. *Inorg. Chem.* **2009**, *48*, 3268−3273. (b) Chen, X.-Y.; Yang, X.; Holliday, B. J. *Inorg. Chem.* **2010**, *49*, 2583−2585. (c) Gee, W. J.; MacLellan, J. G.; Forsyth, C. M.; Moubaraki, B.; Murray, K. S.; Andrews, P. C.; Junk, P. C. *Inorg. Chem.* **2012**, *51*, 8661−8663. (d) Andrews, P. C.; Gee, W. J.; Junk, P. C.; MacLellan, J. G. *Dalton. Trans.* **2011**, *40*, 12169−12179. (e) Peng, J.-B.; Kong, X.-J.; Ren, Y.-P.; Long, L.-S.; Huang, R.-B.; Zheng, L.-S. *Inorg. Chem.* **2012**, *51*, 2186−2190. (f) Zhao, L.; Xue, S.; Tang, J. *Inorg. Chem.* **2012**, *51*, 5994−5996.
(8) Shavaleev, N. M.; Eliseeva, S. V.; Scopelliti, R.; Bünzli, J.-C. G. *Chem.—Eur. J.* **2009**, *15*, 10790−10802.
(9) (a) Borges, A. S.; Dutra, J. D. L.; Freire, R. O.; Moura, R. T.; Da Silva, J. G.; Malta, O. L.; Araujo, M. H.; Brito, H. F. *Inorg. Chem.* **2012**, *51*, 12867−12878. (b) Mao, J.-G. *Coord. Chem. Rev.* **2007**, *251*, 1493−1520.
(10) (a) Whan, R. E.; Crosby, G. A. *J. Mol. Spectrosc.* **1962**, *8*, 315−327. (b) Eliseeva, S. V.; Bunzli, J.-C. G. *Chem. Soc. Rev.* **2010**, *39*, 189−227. (c) Bünzli, J.-C. G.; Chauvin, A.-S.; Kim, H. K.; Deiters, E.; Eliseeva, S. V. *Coord. Chem. Rev.* **2010**, *254*, 2623−2633. (d) Ma, Y.; Wang, Y. *Coord. Chem. Rev.* **2010**, *254*, 972−990.
(11) Freidzon, A. Y.; Scherbinin, A. V.; Bagaturyants, A. A.; Alfimov, M. V. *J. Phys. Chem. A* **2011**, *115*, 4565−4573.
(12) (a) Petit, S.; Baril-Robert, F.; Pilet, G.; Reber, C.; Luneau, D. *Dalton. Trans.* **2009**, 6809−6815. (b) Yuan, N.; Sheng, T.; Tian, C.; Hu, S.; Fu, R.; Zhu, Q.; Tan, C.; Wu, X. *CrystEngComm* **2011**, *13*, 4244−4250. (c) Andrews, P. C.; Deacon, G. B.; Gee, W. J.; Junk, P. C.; Urbatsch, A. *Eur. J. Inorg. Chem.* **2012**, *2012*, 3273−3282. (d) Thielemann, D. T.; Wagner, A. T.; Rösch, E.; Kölmel, D. K.; Heck, J. G.; Rudat, B.; Neumaier, M.; Feldmann, C.; Schepers, U.; Bräse, S.; Roesky, P. W. *J. Am. Chem. Soc.* **2013**, *135*, 7454−7457.
(13) (a) Taxak, V. B.; Kumar, R.; Makrandi, J. K.; Khatkar, S. P. *Displays* **2009**, *30*, 170−174. (b) Liu, S.-L.; Wen, C.-L.; Qi, S.-S.; Liang, E.-X. *Spectrochim. Acta, Part A* **2008**, *69*, 664−669. (c) Kumar, R.; Makrandi, J. K.; Singh, I.; Khatkar, S. P. *J. Lumin.* **2008**, *128*, 1297−1302. (d) Bhaumik, M. L.; Nugent, L. J. *J. Chem. Phys.* **1965**, *43*, 1680−1687. (e) Crosby, G. A.; Whan, R. E.; Freeman, J. J. *J. Phys. Chem.* **1962**, *66*, 2493−2499.
(14) Manseki, K.; Hasegawa, Y.; Wada, Y.; Yanagida, S. *J. Lumin.* **2005**, *111*, 183−189.
(15) (a) Krishnan, P.; Advani, S. G.; Prasad, A. K. *J. Appl. Polym. Sci.* **2012**, *123*, 3331−3336. (b) Krause, M.; Rouleau, A.; Stark, H.; Luger, P.; Lipp, R.; Garbarg, M.; Schwartz, J.-C.; Schunack, W. *J. Med. Chem.* **1995**, *38*, 4070−4079.
(16) Xu, G.; Wang, Z.-M.; He, Z.; Lü, Z.; Liao, C.-S.; Yan, C.-H. *Inorg. Chem.* **2002**, *41*, 6802−6807.
(17) Addamo, M.; Bombieri, G.; Foresti, E.; Grillone, M. D.; Volpe, M. *Inorg. Chem.* **2004**, *43*, 1603−1605.
(18) (a) Kadjane, P.; Charbonnière, L.; Camerel, F.; Lainé, P.; Ziessel, R. *J. Fluoresc.* **2008**, *18*, 119−129. (b) He, P.; Wang, H. H.; Yan, H. G.; Hu, W.; Shi, J. X.; Gong, M. L. *Dalton. Trans.* **2010**, *39*, 8919−8924.
(19) Divya, V.; Freire, R. O.; Reddy, M. L. P. *Dalton. Trans.* **2011**, *40*, 3257−3268.
(20) (a) Puntus, L. N.; Lyssenko, K. A.; Pekareva, I. S.; Bünzli, J.-C. G. *J. Phys. Chem. B* **2009**, *113*, 9265−9277. (b) dos Santos, E. R.; Freire, R. O.; da Costa, N. B.; Paz, F. A. A.; de Simone, C. A.; Junior, S. A.; Araujo, A. A. S.; Nunes, L. A. n. O.; de Mesquita, M. E.; Rodrigues, M. O. *J. Phys. Chem. A* **2010**, *114*, 7928−7936.
(21) (a) Blasse, G.; Bril, A. *J. Chem. Phys.* **1966**, *45*, 3327−3332. (b) Zhang, F. L.; Hou, Y. H.; Du, C. X.; Wu, Y. J. *Dalton. Trans.* **2009**, *0*, 7359−7367.
(22) Xiao, M.; Selvin, P. R. *J. Am. Chem. Soc.* **2001**, *123*, 7067−7073.
(23) (a) Chauvin, A. S.; Gumy, F.; Imbert, D.; Bunzli, J. C. G. *Spectrosc. Lett.* **2007**, *40*, 193−193. (b) Chauvin, A. S.; Gumy, F.; Imbert, D.; Bunzli, J. C. G. *Spectrosc. Lett.* **2004**, *37*, 517−532.
(24) Beeby, A.; M. Clarkson, I.; S. Dickins, R.; Faulkner, S.; Parker, D.; Royle, L.; S. de Sousa, A.; A. Gareth Williams, J.; Woods, M. *J. Chem. Soc., Perkin. Trans. 2* **1999**, 493−504.
(25) (a) He, P.; Wang, H.; Liu, S.; Shi, J.; Wang, G.; Gong, M. *J. Phys. Chem. A* **2009**, *113*, 12885−12890. (b) Binnemans, K. *Chem. Rev.* **2009**, *109*, 4283−4374.
(26) (a) Raj, D. B. A.; Francis, B.; Reddy, M. L. P.; Butorac, R. R.; Lynch, V. M.; Cowley, A. H. *Inorg. Chem.* **2010**, *49*, 9055−9063. (b) Ramya, A. R.; Sharma, D.; Natarajan, S.; Reddy, M. L. P. *Inorg. Chem.* **2012**, *51*, 8818−8826. (c) Divya, V.; Reddy, M. L. P. *J. Mater. Chem. C* **2013**, *1*, 160−170.
(27) (a) Shi, M.; Li, F.; Yi, T.; Zhang, D.; Hu, H.; Huang, C. *Inorg. Chem.* **2005**, *44*, 8929−8936. (b) Jiang, W.; Lou, B.; Wang, J.; Lv, H.; Bian, Z.; Huang, C. *Dalton. Trans.* **2011**, *40*, 11410−11418.
(28) (a) Biju, S.; Reddy, M. L. P.; Cowley, A. H.; Vasudevan, K. V. *J. Mater. Chem.* **2009**, *19*, 5179−5187. (b) Steemers, F. J.; Verboom, W.; Reinhoudt, D. N.; van der Tol, E. B.; Verhoeven, J. W. *J. Am. Chem. Soc.* **1995**, *117*, 9408−9414.
(29) (a) Latva, M.; Takalo, H.; Mukkala, V.-M.; Matachescu, C.; Rodríguez-Ubis, J. C.; Kankare, J. *J. Lumin.* **1997**, *75*, 149−169. (b) Archer, R. D.; Chen, H.; Thompson, L. C. *Inorg. Chem.* **1998**, *37*, 2089−2095. (c) Yang, C.; Fu, L.-M.; Wang, Y.; Zhang, J.-P.; Wong, W.-T.; Ai, X.-C.; Qiao, Y.-F.; Zou, B.-S.; Gui, L.-L. *Angew. Chem., Int. Ed.* **2004**, *116*, 5120−5123. (d) Oxley, D. S.; Walters, R. W.; Copenhafer, J. E.; Meyer, T. Y.; Petoud, S. p.; Edenborn, H. M. *Inorg. Chem.* **2009**, *48*, 6332−6334. (e) Deiters, E.; Gumy, F.; Bünzli, J.-C. G. *Eur. J. Inorg. Chem.* **2010**, *2010*, 2723−2734. (f) Pasatoiu, T. D.; Madalan, A. M.; Kumke, M. U.; Tiseanu, C.; Andruh, M. *Inorg. Chem.* **2010**, *49*, 2310−2315. (g) Divya, V.; Sankar, V.; Raghu, K. G.; Reddy, M. L. P. *Dalton. Trans.* **2013**, *42*, 12317−12323.
(30) Freund, C.; Porzio, W.; Giovanella, U.; Vignali, F.; Pasini, M.; Destri, S.; Mech, A.; Di Pietro, S.; Di Bari, L.; Mineo, P. *Inorg. Chem.* **2011**, *50*, 5417−5429.
(31) (a) Shi, L.; Hong, B.; Guan, W.; Wu, Z.; Su, Z. *J. Phys. Chem. A* **2010**, *114*, 6559−6564. (b) Liu, Y.; Gahungu, G.; Sun, X.; Su, J.; Qu, X.; Wu, Z. *Dalton. Trans.* **2012**, *41*, 7595−7603.
(32) Corrêa, B. A. M.; Gonçalves, A. S.; de Souza, A. M. T.; Freitas, C. A.; Cabral, L. M.; Albuquerque, M. G.; Castro, H. C.; dos Santos, E. P.; Rodrigues, C. R. *J. Phys. Chem. A* **2012**, *116*, 10927−10933.
(33) (a) Tai, C.-K.; Chou, Y.-M.; Wang, B.-C. *J. Lumin.* **2011**, *131*, 169−176. (b) Pérez-Bolívar, C.; Takizawa, S.-y.; Nishimura, G.; Montes, V. A.; Anzenbacher, P. *Chem.—Eur. J.* **2011**, *17*, 9076−9082. (c) Irfan, A.; Cui, R.; Zhang, J. *J. Mol. Struct.: THEOCHEM* **2010**, *956*, 61−65. (d) Shi, Y.-W.; Shi, M.-M.; Huang, J.-C.; Chen, H.-Z.; Wang,

M.; Liu, X.-D.; Ma, Y.-G.; Xu, H.; Yang, B. *Chem. Commun.* **2006**, 1941−1943.
(34) (a) de Mello, J. C.; Wittmann, H. F.; Friend, R. H. *Adv. Mater.* **1997**, *9*, 230−232. (b) Biju, S.; Reddy, M. L. P.; Cowley, A. H.; Vasudevan, K. V. *Cryst. Growth Des.* **2009**, *9*, 3562−3569.
(35) Eliseeva, S. V.; Kotova, O. V.; Gumy, F.; Semenov, S. N.; Kessler, V. G.; Lepnev, L. S.; Bunzli, J.-C. G.; Kuzmina, N. P. *J. Phys. Chem. A* **2008**, *112*, 3614−3626.
(36) Oxford Diffraction, Oxford Diffraction Ltd., Xcalibur CCD system, CrysAlis Software system, version 1.171.34.39, 2010.
(37) Sheldrick, G. M. *SHELXL-97, Program for the Refinement of Crystal Structures*; University of Göttingen: Göttingen, Germany, 1997.
(38) (a) Runge, E.; Gross, E. K. U. *Phys. Rev. Lett.* **1984**, *52*, 997−1000. (b) Becke, A. D. *J. Chem. Phys.* **1993**, *98*, 5648−5652. (c) Lee, C.; Yang, W.; Parr, R. G. *Phys. Rev. B* **1988**, *37*, 785−789.
(39) Dolg, M.; Stoll, H.; Preuss, H. *J. Chem. Phys.* **1989**, *90*, 1730−1734.
(40) Frisch, M. J.; Trucks, G. W.; Schlegel, H. B.; Scuseria, G. E.; Robb, M. A.; Cheeseman, J. R.; Scalmani, G.; Barone, V.; Mennucci, B.; Petersson, G. A.; Nakatsuji, H.; Caricato, M.; Li, X.; Hratchian, H. P.; Izmaylov, A. F.; Bloino, G. Z.; Sonnenberg, J. L.; Hada, M.; Ehara, M.; Toyota, K.; Fukuda, R.; Hasegawa, J.; Ishida, M.; Nakajima, T.; Honda, Y.; Kitao, O.; Nakai, H.; Vreven, T.; Montgomery, J. A., Jr.; Peralta, J. E.; Ogliaro, F.; Bearpark, M.; Heyd, J. J.; Brothers, E.; Kudin, K. N.; Staroverov, V. N.; Keith, T.; Kobayashi, R.; Normand, J.; Raghavachari, K.; Rendell, A.; Burant, J. C.; Iyengar, S. S.; Tomasi, J.; Cossi, M.; Rega, N.; Millam, J. M.; Klene, M.; Knox, J. E.; Cross, J. B.; Bakken, V.; Adamo, C.; Jaramillo, J.; Gomperts, R.; Stratmann, R. E.; Yazyev, O.; Austin, A. J.; Cammi, R.; Pomelli, C.; Ochterski, J. W.; Martin, R. L.; Morokuma, K.; Zakrzewski, V. G.; Voth, G. A.; Salvador, P.; Dannenberg, J. J.; Dapprich, S.; Daniels, A. D.; Farkas, O.; Foresman, J. B.; Ortiz, J. V.; Cioslowski, J.; Fox, D. J. *Gaussian 09*, revision C.01; Gaussian, Inc.: Wallingford, CT, 2010.
(41) (a) Habenschuss, A.; Spedding, F. H. *J. Chem. Phys.* **1980**, *73*, 442−450. (b) Gospodinov, G. G.; Stancheva, M. G. *J. Therm. Anal. Calorim.* **1999**, *55*, 221−226. (c) Yang, C.; Liu, L.; Gao, Y.; Zhang, W.; Zhang, X.; Zhang, L. *Luminescence* **2006**, *21*, 98−105.